



This is a repository copy of *A theoretical description of a multi-source energy harvester*.

White Rose Research Online URL for this paper:
<http://eprints.whiterose.ac.uk/140265/>

Version: Accepted Version

Proceedings Paper:

Gosliga, J. and Wagg, D.J. orcid.org/0000-0002-7266-2105 (2018) A theoretical description of a multi-source energy harvester. In: Sensors and Instrumentation, Aircraft/Aerospace and Energy Harvesting. 36th IMAC, A Conference and Exposition on Structural Dynamics 2018, 12-15 Feb 2018, Orlando, USA. Conference Proceedings of the Society for Experimental Mechanics Series, 8 . Springer , pp. 41-47. ISBN 978-3-319-74641-8

https://doi.org/10.1007/978-3-319-74642-5_5

© 2019 The Society for Experimental Mechanics, Inc. This is an author produced version of a paper subsequently published in Sensors and Instrumentation, Aircraft/Aerospace and Energy Harvesting , Volume 8. Uploaded in accordance with the publisher's self-archiving policy.

Reuse

Items deposited in White Rose Research Online are protected by copyright, with all rights reserved unless indicated otherwise. They may be downloaded and/or printed for private study, or other acts as permitted by national copyright laws. The publisher or other rights holders may allow further reproduction and re-use of the full text version. This is indicated by the licence information on the White Rose Research Online record for the item.

Takedown

If you consider content in White Rose Research Online to be in breach of UK law, please notify us by emailing eprints@whiterose.ac.uk including the URL of the record and the reason for the withdrawal request.



eprints@whiterose.ac.uk
<https://eprints.whiterose.ac.uk/>

The theory of a prototype multi-source energy harvester

J. Gosliga*and D. J. Wagg

Department of Mechanical Engineering, University of Sheffield, S1 3JD, UK

October 19, 2017

Abstract

By harvesting energy from more than one source, it is possible to improve the power output from an energy harvester. In this paper we present an analysis that allows the maximum power absorbed by a multi-source harvester to be found. This is based on an extension to analysis that was previously used to derive a power bound for a single source mechanical energy harvester driven by stochastic vibration. Firstly, a single source power bound is derived for a system with thermo-electrical coupling, driven by stochastic time-varying temperature gradients. This power bound is verified using numerical simulations carried out in MATLAB. This analysis is then extended to a system with thermo-electro-mechanical coupling, driven by both fluctuating temperature gradients and mechanical vibration. It is shown that the resulting power bound is the sum of the maximum power absorbed by the thermal system and the mechanical system. As this power bound is greater than that for a single source system, it demonstrates that a system driven by multiple sources has the potential to absorb more power than a system driven by a single source.

1 Introduction

Energy harvesting is a process for converting energy from one form into another, more useful form. Previously this was done with harvesters that could only convert from one form of energy. However, devices that can convert from multiple sources are now being explored as they can achieve a greater power output for the same size device. There are two main types, harvesters that use multiple methods to enhance the output from a single source and harvesters that harvest from multiple distinct sources. This paper will define a true multi-source harvester as one that utilises multiple distinct sources. As there are a huge number of possible theoretical combinations, in this paper the scope is restricted to devices using some combination of the piezoelectric and pyroelectric effects.

One of the first hybrid devices of this type used shape-memory alloys in combination with dielectric materials so that piezoelectric and pyroelectric effects could be combined to enhance the amount of energy harvested from a single thermal source [3]. Piezoelectric and pyroelectric effects were combined to enhance the output from a triboelectric generator in [5]; despite using multiple effects, this device still only harvests energy from a single mechanical source. The combination of tribo/piezo/pyro-electric effects was also used in a device [4] to harvest energy from independent mechanical and thermal sources at the same time, making this a true multi-source harvester. In this paper we will explore a device which harvests from both mechanical and thermal source by utilising the piezoelectric and pyroelectric effects.

The upper limit on the power that an energy harvester can absorb is a useful method for benchmarking devices, as this will be the limit to how much useful power they can generate. This number does not depend on the efficiency of the device, and merely represents how much energy is available to a device. By comparing the upper limits on the power absorbed, it can be shown that there is more power available when harvesting from multiple sources. There already exists a power bound for a piezoelectric harvester driven by mechanical vibration [2]. Since no such bound exists for a pyroelectric harvester, in Section 2, it is necessary to derive an expression for the power absorbed by a pyroelectric harvester driven by stochastically varying temperatures. In Section 2.1, this expression will be verified through numerical simulations. Finally, in

*Address all correspondence to this author jsgosliga1@sheffield.ac.uk.

Section 3, we will derive an expression for the power absorbed by the full harvester from both a mechanical and a thermal source.

2 Deriving a bound on the power absorbed by a pyroelectric system

The theoretical power bound for a mechanical harvester using piezoelectric materials with stochastic vibrational input has been shown to be

$$P = \frac{\pi S_{0x} m}{2}. \quad (1)$$

as demonstrated in [2]. P represents the power absorbed by the device; S_{0x} is the amplitude of the power spectral density of the input vibrations; and m is the total mass of the device. This bound has been shown to be valid for piezoelectric devices in [1], however it has not been extended to pyroelectric devices. Since pyroelectric devices are driven by a temperature gradient which creates a potential rather than a displacement, the analysis will differ from that presented by [2] or [1]. Furthermore, the coupling between the voltage and temperature gradient is not the same as the electromechanical coupling found in piezoelectrics.

The state equations for a pyroelectric device in an equilibrium state are as follows

$$C_s \ddot{\theta} + R_s \dot{\theta} - p \dot{u} = 0 \quad (2)$$

$$C_v \ddot{u} + R_v^{-1} \dot{u} + p \ddot{\theta} = 0, \quad (3)$$

where C_v is the electrical capacitance; R_v is the electrical resistance; C_s is the analogous thermal capacitance; R_s is the analogous thermal resistance; θ is the temperature difference between the device and the surroundings with reference to an equilibrium state; $\dot{u} = v$ where v is the instantaneous voltage; and p represents the pyroelectric coupling coefficient.

To write these equations in a state-space form we need to eliminate the second-order term $\ddot{\theta}$ in Eq. (3). So it is necessary to substitute in Eq. (2) into (3). This gives

$$C_v \ddot{u} + (R_v^{-1} + p^2 C_s^{-1}) \dot{u} - p R_s C_s^{-1} \dot{\theta} = 0. \quad (4)$$

We can now introduce c which represents the temperature difference between the heat source and the surroundings. This difference is assumed to fluctuate in such a way that it is equivalent to a stationary white-noise input such that $E[\ddot{c}(t)\ddot{c}(t+\tau)] = \pi S_{0\theta} \delta(\tau)$, where $S_{0\theta}$ is the amplitude of the power spectral density of the temperature fluctuations of the heat source, and δ is the value of the Dirac delta function at time τ . This gives us a pyroelectric system which is driven by a stochastically varying thermal gradient as represented by

$$C_s \ddot{\theta} + R_s \dot{\theta} - p \dot{u} = C_s \ddot{c}. \quad (5)$$

where the term on the right-hand side represents an entropy flow into the system.

These can be combined and expressed in a form describing the state of the coupled system and the outputs

$$\dot{x} = Ax + G\zeta(t), \quad (6)$$

where the coefficients for the state-space variables are

$$A = \begin{pmatrix} 0 & 1 & 0 & 0 \\ 0 & -C_s^{-1}R_s & 0 & -pC_s^{-1} \\ 0 & 0 & 0 & 1 \\ 0 & pC_s^{-1}C_s^{-1}R_q & 0 & -C_v^{-1}(R_v^{-1} + p^2C_s^{-1}) \end{pmatrix}. \quad (7)$$

If we assume $\tau = 0$, then $E[\ddot{c}(t)^2] = \pi S_{0\theta} E[\zeta(t)^2]$ and so $\ddot{c}(t) = \sqrt{\pi S_{0\theta}} \zeta(t)$. This results in the input matrix

$$G = \begin{pmatrix} 0 \\ \sqrt{\pi S_{0\theta}} \\ 0 \\ 0 \end{pmatrix}. \quad (8)$$

If we introduce an augmented mass matrix,

$$M = \begin{pmatrix} 0 & 0 & 0 & 0 \\ 0 & C_s & 0 & 0 \\ 0 & 0 & 0 & 0 \\ 0 & 0 & 0 & C_v \end{pmatrix}, \quad (9)$$

then we can express the power absorbed by the coupled system in a similar fashion to [2], which gives

$$P = (1/2)\text{Tr}[MGG^T], \quad (10)$$

where Tr is the trace of the resultant matrix. Therefore

$$P = (1/2)\text{Tr} \begin{bmatrix} 0 & 0 & 0 & 0 \\ 0 & \pi S_{0\theta} C_s & 0 & 0 \\ 0 & 0 & 0 & 0 \\ 0 & 0 & 0 & 0 \end{bmatrix}, \quad (11)$$

which in this case leads to the following expression for the maximum power absorbed by the pyroelectric system

$$P = \frac{\pi S_{0\theta} C_s}{2}. \quad (12)$$

2.1 Numerical simulation of the pyroelectric system

In order to verify the analytical results, a numerical simulation of the system was carried out. The system described by Eqs. (4) and (5) was excited by a fluctuating temperature gradient, such as that shown in Fig. 1. The results in Fig. 2, show that the absorbed by the system increases linearly with C_s the thermal capacitance. The numerical results for the power absorbed match the power bound predicted by Eq. (12). Also included in the figure is total power dissipated. This is the sum of the power dissipated by the resistor and as entropy through the thermal resistance. Since the power dissipated can never exceed the power absorbed, the total power lost by the system is limited by Eq. 12.

The parameter values used in the simulation are $S_{0\theta} = 2 \times 10^{-3} \pi^{-1} \text{ } ^\circ K^2/s$; $C_v = 1 \times 10^{-6} F$; $R_v = 1 \times 10^6 \Omega$; $p = 1 \times 10^{-10}$ $R_s = 1 \times 10^6 \text{ } ^\circ K^2/W$; and C_s was varied between $1 \times 10^{-2} J/^\circ K^2$ and $1 \times 10^{-4} J/^\circ K^2$. In the thermal simulation, the expression for the power absorbed from the varying temperature gradient is

$$P = E[C_s \ddot{c} \dot{\theta}] \quad (13)$$

and the amount of power that is dissipated is given by

$$P = E[R_s^{-1} \dot{\theta}^2] + E[R_v^{-1} \dot{u}^2]. \quad (14)$$

3 Deriving a power bound for a multi-source electro-mechanical system

Now that we have found the state equations for a pyroelectric system, we can combine these with the equations for a piezoelectric system. In this way, we can derive a power-bound for a system driven by both thermal and mechanical energy. This will also allow us to examine a system with multiple outputs rather than a single output.

We will consider a system in which a single piece of dielectric material—displaying both pyroelectric and piezoelectric effects—experiences both varying mechanical displacement and fluctuating thermal gradients. This dielectric material is then connected to a simple resistor-capacitor (RC) circuit, representing the harvesting circuitry. The system can be described using the following system of coupled equations

$$m\ddot{y} + \gamma\dot{y} + ky + d\dot{u} = -m\ddot{b}, \quad (15)$$

$$C_s\ddot{\theta} + R_s\dot{\theta} - p\dot{u} = C_s\ddot{c} \quad (16)$$

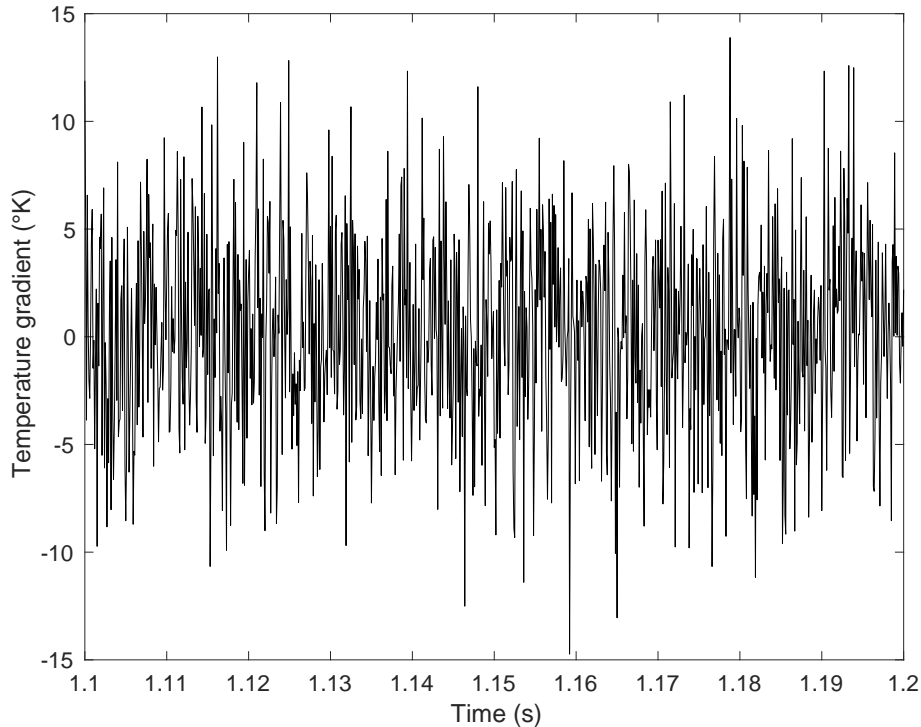


Figure 1: A 0.1s sample of the time history of the stochastically varying input temperature gradient c

$$C_v \ddot{u} + (R_v^{-1} + p^2 C_s^{-1}) \dot{u} - p R_s C_s^{-1} \dot{\theta} - d \dot{y} = 0. \quad (17)$$

where Eq. (15) represents a mechanical system with mass m , damping coefficient γ and stiffness k . These equations were derived in a similar fashion to Eqs. (5) and (4).

This system is being driven not only by vibration, but also by some form of stochastically varying temperature difference. Since these equations represent a dielectric system, there is an piezoelectric electromechanical coupling term d and a pyroelectric thermo-electrical coupling term p . Therefore thermal energy into the system can either remain as thermal energy, or convert into electrical or mechanical energy. The same goes for any mechanical energy into the system. The flow of energy in the system is demonstrated in Fig. 3.

Energy in the system can be dissipated through mechanical damping or as entropy or dissipated through the resistor. The amount of energy dissipated in each case is determined by the damping coefficient γ , the thermal resistance R_s , or the electrical resistance R_v , respectively. In this system, we consider that the resistor and other circuitry are separated from the dielectric material. This means that heat dissipated through the resistor can be considered lost to the environment and does not feed back into the thermal system. We also consider that the mechanical damping dissipates energy in such a fashion that this is also completely lost to the environment.

It is assumed that both the motion of the base, b , and the fluctuation of the temperature gradient, c , can be approximated as stationary white-noise processes, such that

$$\mathbb{E}[\ddot{b}(t)\ddot{b}(t + \tau)] = \pi S_{0x} \delta(\tau), \quad (18)$$

$$\mathbb{E}[\ddot{c}(t)\ddot{c}(t + \tau)] = \pi S_{0\theta} \delta(\tau). \quad (19)$$

The separate coupled Eqs. (15), (16) and (17), can be combined using generalised state-space variable

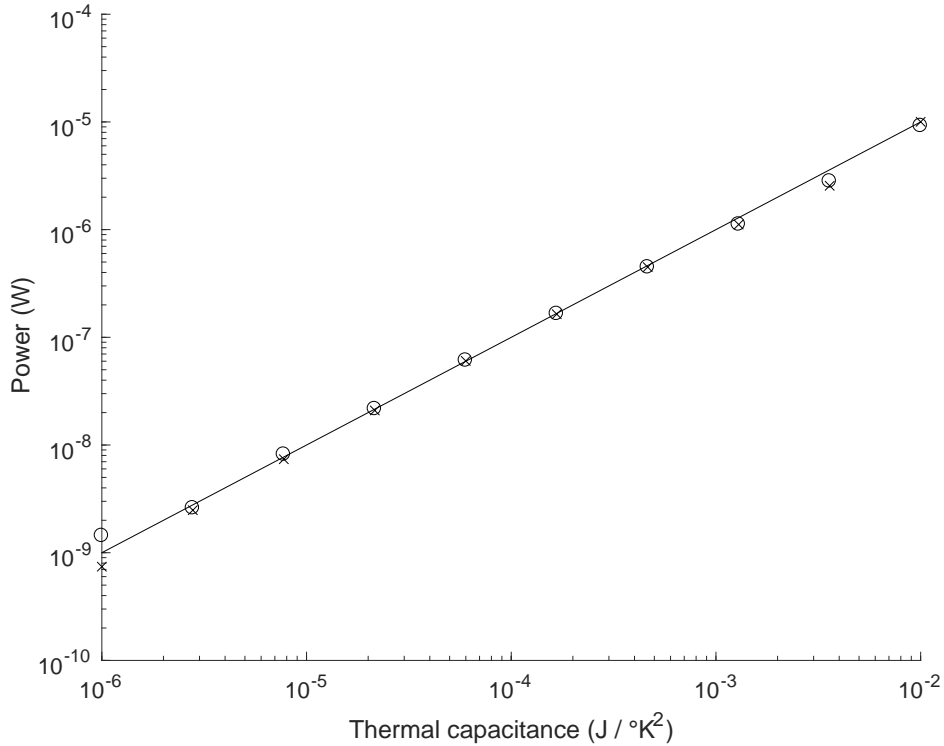


Figure 2: The solid line (orange) shows the linear increase in power from increasing thermal capacitance, where the power spectral density of the fluctuating temperature $S_{0\theta}$ and other system parameters are held constant. It can be seen that the power absorbed (marked by crosses) from the stochastically varying temperature gradient c is equal to the total power dissipated by the system (marked by circles)

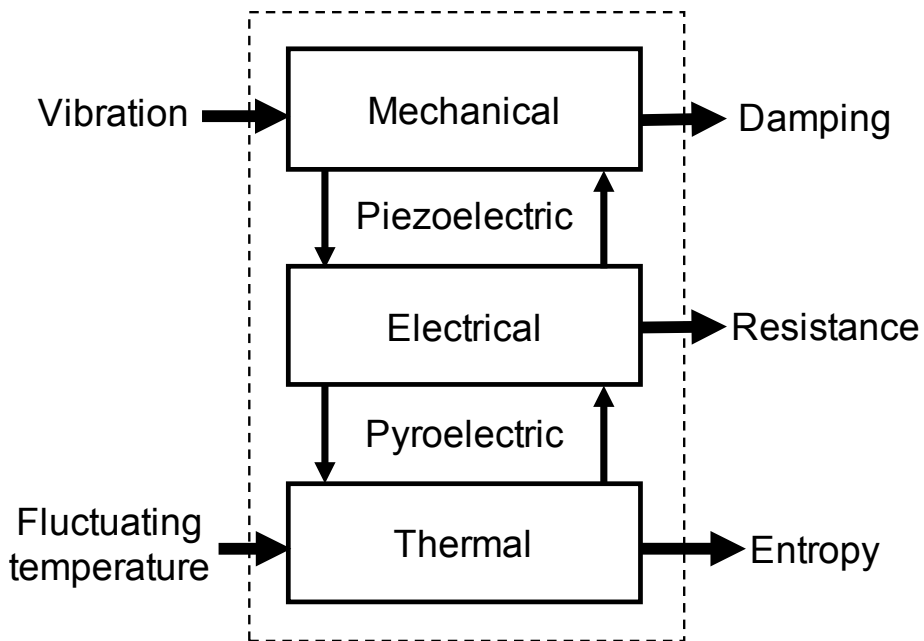


Figure 3: A schematic of the system showing arrows into the dashed box representing energy absorbed by the system from both vibrations and fluctuating temperatures. Energy is transferred within the system via the piezoelectric and pyroelectric effect. Arrows out of the system (dashed box) represent energy dissipated through the damping, and electrical and thermal resistance

x to describe the displacement y , the temperature gradient θ and voltage u where

$$x = \begin{pmatrix} y \\ \dot{y} \\ \theta \\ \dot{\theta} \\ u \\ \dot{u} \end{pmatrix}. \quad (20)$$

The new equation describing the state of the coupled system and the outputs then becomes

$$\dot{x} = Ax + G\zeta(t), \quad (21)$$

where the coefficients for the state-space variables are

$$A = \begin{pmatrix} 0 & 1 & 0 & 0 & 0 & 0 \\ -m^{-1}k & -m^{-1}\gamma & 0 & 0 & 0 & -m^{-1}d \\ 0 & 0 & 0 & 1 & 0 & 0 \\ 0 & 0 & 0 & -pC_s^{-1}R_s & 0 & -C_s^{-1} \\ 0 & 0 & 0 & 0 & 0 & 1 \\ 0 & pC_v^{-1}d & 0 & C_v^{-1}C_s^{-1}R_s & 0 & -p^2C_v^{-1}(R_v^{-1} + C_s^{-1}) \end{pmatrix} \quad (22)$$

and the input matrix

$$G = \begin{pmatrix} 0 \\ -\sqrt{\pi S_{0x}} \\ 0 \\ \sqrt{\pi S_{0\theta}} \\ 0 \\ 0 \end{pmatrix}. \quad (23)$$

Again we can introduce an augmented mass matrix

$$M = \begin{pmatrix} 0 & 0 & 0 & 0 & 0 & 0 \\ 0 & m & 0 & 0 & 0 & 0 \\ 0 & 0 & 0 & 0 & 0 & 0 \\ 0 & 0 & 0 & C_s & 0 & 0 \\ 0 & 0 & 0 & 0 & 0 & 0 \\ 0 & 0 & 0 & 0 & 0 & C_v \end{pmatrix}. \quad (24)$$

Using this augmented matrix M , we can express the power absorbed by the coupled system in a similar way to that derived previously

$$P = (1/2)\text{Tr}[MGG^T], \quad (25)$$

where Tr is the trace of the resultant matrix. Therefore

$$P = (1/2)\text{Tr} \begin{bmatrix} 0 & 0 & 0 & 0 & 0 & 0 \\ 0 & \pi S_{0x}m & 0 & 0 & 0 & 0 \\ 0 & 0 & 0 & 0 & 0 & 0 \\ 0 & 0 & 0 & \pi S_{0\theta}C_v & 0 & 0 \\ 0 & 0 & 0 & 0 & 0 & 0 \\ 0 & 0 & 0 & 0 & 0 & 0 \end{bmatrix}, \quad (26)$$

which in this case leads to the following expression for the combined maximum power

$$P = \frac{\pi S_{0x}m}{2} + \frac{\pi S_{0\theta}C_v}{2}. \quad (27)$$

This theoretical limit for a system with multiple sources appears to be the sum of Eqs. (1) and (12), which describe the thermal power bound and the mechanical power bound respectively.

4 Conclusion

The aim of this paper was to explore devices which utilise multiple sources of energy in order to improve output. Upper limits on the power that a harvester could absorb were used as it provides a measure with which to benchmark devices. If the upper limit of a theoretical device that harvests from multiple sources is greater than that for a single source, then it represents a potential improvement. In order to compare the upper limits for a multi-source harvester, it was necessary to find limits for different energy types. In this case, a limit on the amount of thermal energy that could be harvested using the pyroelectric effect was found. This showed that the same theoretical framework used to find the limit for a mechanical harvester could be extended to different types of harvester. Once the limit for a pyroelectric harvester had been found, the expression was validated using a numerical simulation. The equations of state for a system with inputs from multiple sources were then derived. This system used both the piezoelectric and the pyroelectric effect in combination. This allowed for both mechanical and thermal energy to be converted into electrical energy. A similar state-space analysis was carried out on these equations. This combined system was found to have an upper limit on the power absorbed that was the sum of the power-bounds for the mechanical and thermal systems individually. This demonstrates that there is more power available to this type of multi-source harvester than the single source harvesters.

It is believed that this theoretical framework can be extended to harvesters of other forms of energy, so that the maximum possible power available in a given environment can be quantified. As a result it would be possible to make a systematic comparison of which combination of energy sources would provide the most potential power in a given system.

References

- [1] D. Hawes. *Nonlinear Stochastic Vibration Analysis for Energy Harvesting and Other Applications*. PhD thesis, University of Cambridge, 2016.
- [2] R. S. Langley. A general mass law for broadband energy harvesting. *Journal of Sound and Vibration*, 333(3):927–936, 2014.
- [3] D. Zakharov, B. Gusarov, E. Gusarova, B. Viala, O. Cugat, J. Delamare, and L. Gimeno. Combined Pyroelectric, Piezoelectric and Shape Memory Effects for Thermal Energy Harvesting. *Journal of Physics: Conference Series*, 476(1):012021, 2013.
- [4] H. Zhang, S. Zhang, G. Yao, Z. Huang, Y. Xie, Y. Su, W. Yang, C. Zheng, and Y. Lin. Simultaneously Harvesting Thermal and Mechanical Energies based on Flexible Hybrid Nanogenerator for Self-Powered Cathodic Protection. *ACS Applied Materials and Interfaces*, 7(51):28142–28147, 2015.
- [5] Y. Zi, L. Lin, J. Wang, S. Wang, J. Chen, X. Fan, P. K. Yang, F. Yi, and Z. L. Wang. Triboelectric-pyroelectric-piezoelectric hybrid cell for high-efficiency energy-harvesting and self-powered sensing. *Advanced Materials*, 27(14):2340–2347, 2015.